A Simplified Sub-Surface Soil Salinity estimation using Synergy of Sentinel-1 SAR and Sentinel-2 multispectral satellite data, for early stages of wheat crop growth in Rupnagar, Punjab, India

Akshar Tripathi[1] and Reet Tiwari[1]

[1]Indian Institute of Technology Ropar

August 28, 2020

Abstract

Soil salinity has today become a highly disastrous phenomenon that is responsible for crop failure worldwide and specially in countries with low farmer incomes and food insecurity. Soil salinity is often caused due to water accumulation in fields due to unscientific flood irrigation wherein plants intake the water leaving salts behind. It is, however, the sub-surface soil salinity that affects the plant growth. These salts in sub-surface soil get trapped in root nodules of plants and prevent further water intake. There have been very few studies conducted for sub-surface soil salinity estimation. Hence this study aims to estimate sub-surface soil salinity (at 60 cm depth) for early stage of wheat crop growth in a simplified manner using freely available satellite data, which is a novel feature and prime objective in this study. The study utilizes Sentinel-1 SAR (Synthetic Aperture RADAR) data for backscatter coefficient generation, Sentinel-2 multispectral data for NDSI (Normalised Differential Salinity Index) generation and on ground equipment for direct collection of soil electrical conductivity. The data were collected for two dates in November and December 2019 and one date for January 2020 during the early stage of wheat crop growth. The dates were selected keeping in mind the satellite pass over the study area of Rupnagar on the same day. Ordinary Least Squares regression was used for modelling which gave R2-statistics of 0.99 and 0.958 in training and testing phase and root mean square error of 1.92 in modelling for soil salinity estimation.

1. Introduction

Soil salinity is defined as the accumulation of salts in the soil (Rengasamy, 2010). Soil salinity is a major environmental catastrophe caused by both natural and anthropogenic reasons (Rapp, 1986). Nearly 20% of all land globally is salinity affected and has raised huge concerns for governments bodies worldwide to introduce timely land reclamation measures (Ringler, Bhaduri, & Lawford, 2013). Land reclamation for salinity affected areas requires timely monitoring of salinity status of soil and its indicators in an efficient manner to curb the causative factors (Vogt et al., 2011). Though not as damaging initially as other hazards like earthquake, volcanic eruption or floods, soil salinity can take a heavy toll on lives in the long run (Dumanski Samuel Pieri, Christian Agriculture and Agri-Food Canada, 1998).

Today food security is a highly debated topic and with increasing salinity in soil for areas which depend upon artificial irrigation sources, soil salinity is causing stunted plant growth and crop failure at times (García-Tejero, Durán-Zuazo, Muriel-Fernández, & Rodríguez-Pleguezuelo, 2011; Koevoets, Venema, Elzenga, & Testerink, 2016).

Increase in soil salinity causes decrease in moisture intake capacity of plants since their root nodules get blocked by salts (Egamberdieva, Li, Lindström, & Räsänen, 2016; Etehadnia, Waterer, De Jong, & Tanino, 2008; Franzini, Azcón, Ruiz-Lozano, & Aroca, 2019). Moreover, high concentration of salts in water causes reverse osmosis resulting in the wilting of plants causing their perishing(Arora et al., 2018). This in turns affects the crop yield and causes heavy loss to farmers. Salinity in soil happened mainly due to natural causes such as frequent flooding but over the years, unscientific and improper irrigation management(Baig & Shahid, 2014). Figures indicate that the soil salinity has become a highly serious phenomenon. Primary salinity affected areas globally account for 955 M ha and secondary salinity affected areas are some 77 M ha and out of these 58% is irrigated area that shows the major cause of salinity is anthropogenic(Amin, 2004).

Increasing human population and the competition for resources has posed a heavy threat on all-natural resources including water and soil (Cassman, Dobermann, Walters, & Yang, 2003). Since soil supports almost all life on earth, proper management of soil in a scientific way becomes very important (Miltner, Bombach, Schmidt-Brücken, & Kästner, 2012). Salinity can occur out of a number of other factors apart from improper irrigation- engineering problems, soil erosion and soil dispersion(Qadir, Ghafoor, & Murtaza, 2000). For areas with a history of water logging, the soil salinity becomes more acute(Bhutta & Smedema, 2007; Shah, Molden, Sakthivadivel, & Seckler, 2001). The plants intake the moisture leaving behind the dissolved salts in water(Konukcu, Gowing, & Rose, 2006). After a period of time, this salt accumulates around the root nodules making further water intake impossible(Streeter & Wong, 1988). Salinity in soil can be determined by estimating the electrical conductivity of soil(Rhoades, Shouse, Alves, Manteghi, & Lesch, 1990; Rhoades & van Schilfgaarde, 1976). The electrical conductivity measured in milli-siemens per meter is a measure of the ionic concentration of the soil (Susha et al., 2018).

In agriculture science, soil is considered to be saline in conditions when there is sufficient amount of salts dissolved in root zone soil moisture to adversely affect the plant growth (Rengasamy, Chittleborough, & Helyar, 2003). Some studies claim soils to be saline in cases when soil electrical conductivity is more than $4dSm^{-1}$ at 25°C (Igartua, Gracia, & Lasa, 1994). Different plants have different tolerance for soil salinity levels beyond which their growth is adversely affected, as shown in Table 1(Xie et al., 2009)-

Table 1 . GENERAL SOIL SALINITY TOLERANCE RATE FOR PLANTS

SALINITY IN TERMS OF ELECTRICAL CONDUCTIVITY ($EC=dSm^{-1}$)	PLANT RESPONSE
0-2	Mostly negligible
2-4	Growth of Sensitive plants is affec
4-8	Growth of many plants is affected
8-16	Only tolerant plants grow effectiv
Above 16	Only few very tolerant plants gro

The above table shows that in coastal regions specially where there is regular accumulation of sea water in high tides, only few exotic plant species with high salinity tolerance levels can thrive well.

Increased soil salinity not only causes less water intake in plants but also leads to acute nutrient imbalances (Hu & Schmidhalter, 2005). This often causes toxins detrimental for plant growth to accumulate and reduction in water infiltration in the event of high sodium ion (Na^+) concentration(Qadir & Schubert, 2002). Statistics reveal that globally about 1 billion hectares, close to 7% of earth's continental crust is salinity affected (Lewis & Maslin, 2015). Soil salinity can occur in any soil type anywhere on earth. However, semi-arid and arid regions are the worst affected (Jordán, et al., 2004). Soil salinity depends upon (Jolly, McEwan, & Holland, 2008)-

Salt could be found along with parent material like rock or salt layers accumulated over time.

Leaching and weathering of parent rock materials causes the free ion accumulation in soil thereby increasing soil salinity.

During erosion by wind or water, soil salinity can occur by materials brought by erosive forces from one area to another.

In case when the underground water becomes saline due to prolonged leaching, the places where the water table is near the surface soil becomes saline after long spells of dryness and evaporation from surface.

Most common cause of soil salinity is however the unscientific flood irrigation. The irrigation water from tube-wells or canals if containing dissolved salts often leads to soil salinity or increase in the salinity levels of soil. Remote sensing is a non-evasive and time saving tool which can be applied effectively for monitoring of soil salinity levels and mapping of salinity affected areas (Katsaros, Vachon, Liu, & Black, 2002). Since many decades and ever since the inception of remote sensing as an advanced surveying tool with launch of first remote sensing satellite- Landsat-1 in early 1970s; spaceborne remote sensing found extensive use in agriculture (Zhang et al., 2002). However, there was still paucity of dedicated use of spaceborne remote sensing for soil health studies (Pampaloni & Calvet, 2007; Wagner, Lemoine, & Rott, 1996). Initial soil health studies were done in conjunction with remote sensing research for precision agriculture using optical multispectral satellite datasets (Viterbo & Betts, 1999; Y. Xie, Sha, & Yu, 2008). Since the optical, thermal, and hyperspectral datasets have their own constraints owing to their non availability every time and in all seasons due to dense cloud covers specially in monsoon months, a need for all weather data was felt (Kim & Hong, 2007). It was due to this that microwave or Synthetic Aperture RADAR (SAR) remote sensing came into use (Hong & Pan, 2000). It has a penetration ability and being an active sensor, it has high temporal resolution with 24-hour data availability (Holmes, 1959; Liu et al., 2011). Apart from this, owing to its several modelling and decomposition approaches, it becomes the most versatile branch of remote sensing research (Engman, 1991; Larson et al., 2010). But spaceborne remote sensing has its own limitations (Pachepsky, Guber, & Jacques, 2005). High resolution optical datasets are mostly available on commercial and paid basis and almost all currently active SAR Datasets are available at very high costs (Delaney, 1974; Walker, Houser, & Willgoose, 2004). This often causes budgetary constraints on advanced research. Hence a cost-effective study is needed to carry out research that is feasible and at par with those conducted using commercial data. Moreover, SAR data has lots of speckle noise which is absent in optical data (Chong & T, 2005). Keeping all the limitations and constraints in view, this study was conducted using synergy of both optical and SAR remotely sensed and freely available high temporal resolution satellite data for soil salinity estimation and modelling. This study uses backscatter coefficients generated after calibrating the SAR data from Sentinel-1 checks their sensitivities for soil moisture and electrical conductivity values collected from ground along with NDSI calculated from Sentinel-2 optical multispectral data of the same dates (David R . Anderson, 2000; Pope & Webster, 1972). Also, surface temperature data in Fahrenheit was also used using a thermal imager on ground during field data collection (Congalton, Fenstermaker, & Mcgwire, 1991; Richardson & Hollinger, 2005). This study is unique in the sense that it uses a multisensor remote sensing approach along with a synergy of field data to be fed into developing a Ordinary Least Squares (OLS) model for estimation of soil salinity (Dekker, 1998; Sowter et al., 2016).*1.1 Short Literature review*Remote sensing is defined as the science and art of data collection, processing, interpretation, and analysis of data from a distance without coming in actual tangible contact with the target object (Guzha, 2004; Metternicht & Zinck, 2003). In optical remote sensing, the target is illuminated by the Sun's rays and the reflectance is captured by the sensors of the satellite operating in narrow band ranges of the electromagnetic spectrum and capture imagery in several wavelength band ranges (Herrick, 2000; Stenberg, Rossel, Mouazen, & Wetterlind, 2010; K. T. (eds). 2013 Wymann von Dach S, Romeo R, Vita A, Wurzinger M, 2014). In microwave remote sensing, the sensor being an active sensor, illuminates the target with emitted electromagnetic waves in the microwave region (Raina, Joseph, & Haribabu, 2010; K. T. (eds). Wymann von Dach S, Romeo R, Vita A, Wurzinger M, n.d.). The waves are received back after interaction with the target and are received on the receiver of the sensor platform which generates an image of the target object (Braidwood, 1960; Muir, Pretty, Robinson, Thomas, & Toulmin, 2010). Remote sensing data is collected from a variety of sensors like visible and infrared sensors, optical and thermal imaging sensors, hyperspectral sensors and microwave sensors and based on the respective behavioural properties of salinity effected areas with the incident radiation, mapping of soil salinity is done (Schmugge et al., 2002). In remote sensing applied to land resource surveys, wavelengths between 0.4-1.5mm are most used (Aslan et al., 2016). Landsat TM (Thematic Mapper) and SPOT were the satellites that found usage widespread for natural resource mapping for landscapes spread over hectares of land (Akshar Tripathi, 2018). The image type depended upon not only the purpose but also on the sensor used and the number of spectral bands it offered (Lobell et al., 2015), with Landsat providing much greater number of spectral bands than SPOT. Landsat images were used for classification, both supervised and unsupervised (Dengsheng Lu, Tian, Zhou, & Ge, 2008). Multispectral bands 3,4,5 is used along with TM bands 7 for the proper mapping of salinity effected soils as described by (Hari Shanker Srivastava et al., 2008). Davidson & Finlayson, 2007; Mahlke, 1996**,** used synergy of thermal and microwave remotely sensed data and used RADAR backscatter for fresh and saline water and surface temperature as parameters to model for soil salinity. (Leckie, 1984) found that Landsat bands 1-5 and 7 are sensitive for soil minerals and are good for mapping when salinity causing minerals are dominant in soil also soil salinity affects the thermal properties of the soil. (Anderson & Croft, 2009) used Landsat MSS data to produce maps for calcareous, gypsiferous and clayey soils and also found the TM bands helpful when used with aerial photographs for arid and semi-arid regions (Mougenot, Pouget, & Epema, 1993). Sharma, Saxena, & Verma, 2000 used topographic survey maps and standard False colour composite from Landsat MSS imagery to map saline and non-salinity affected areas. Saha, Kudrat, & Bhan, 1990**,** used digital image classification using Landsat data and successfully mapped saline, non-saline and moderately saline areas which were waterlogged for a long period of time, with 96% accuracy in classification. Similar classification study was done by D Lu & Weng, 2007. Calvão & Palmeirim, 2004 used band rationing and proved that in Middle to Near Infrared bands from Landsat were useful in mapping chlorosis affected soils. Mougenot et al., 1993**,** used thermal infrared band and found that the hygroscopic properties of soil can be analysed and the reflectance from leaves of plants depends upon the chemical composition of the dissolved salts in the up taken water and morphology of plant. Hansen, Dubayah, & Defries, 1996, found classification tree was useful when Normalised Differential Vegetation Index (NDVI) is used along with brightness index for mapping of soil salinity affected areas in Morocco and Pakistan Respectively. Ahmed & Luis, 2010, used multiple regression analysis using electrical conductivity values from field and based on that generated a soil salinity map for entire Mexico. Mayaux et al., 2004 used NDVI and Surface Energy Balance Algorithm for Land (SABAL) to map and classify the soils based on the various salinity levels. It is clear from the studies above that most of the soil salinity studies conducted were of qualitative classification and mapping based. There are only few dedicated studies for soil salinity estimation and modelling using multiple remote sensing sensors in a quantitative way. Most of the studies conducted for soil salinity estimation using remotely sensed data have been done at surface level since remote sensing is a surface phenomenon. But after going through literature, it was found that it is the sub-surface soil salinity that affects the plant growth as the salts underneath get trapped in root nodules and prevent further moisture intake by plants. This study is one of the few studies which estimate soil salinity in terms of electrical conductivity using remotely sensed SAR and optical data in synergy with field data. Apart from this, it was also aimed to provide a simple and robust soil salinity estimation approach, in this study. Early stage of wheat crop growth was chosen owing to the presence of more exposed area of soil to the satellite sensor during it pass. Moreover, C-band satellite data from Sentinel-1 cannot penetrate the vegetation cover once the crop matures. Hence study of soil becomes difficult.*1.2 Electrical Conductivity as Soil Salinity Indicator*The amount of electrical current that a material allows to pass through it, or the current carrying capacity of a material is defined as its electrical conductivity(Frackowiak, 2001). Electrical conductivity is also known as specific conductance and is measured in $mS.m^{-1}$ (milli Siemens per meter)(Riffat & Ma, 2003). Electrical conductivity of soil correlates with soil properties like soil texture, cation exchange capacity, salinity, as a measurement of current conducting capacity of soil (Landauer, 1978). Since soil salinity refers to the concentration of ions in the soil pore water that make the further water up take difficult, the laboratory determination of soil salinity is a cumbersome process which is time taking(Corwin & Lesch, 2003). Electrical conductivity measurement as an indicator of soil salinity is an effective and time saving method for soil salinity estimation(Rhoades, 1993). The cause of the electrical conductivity is the ions present in the soil which become more loosely bound to the soil pores in presence of moisture owing to the high dielectric constant of water (Corwin & Lesch, 2005). The ions get aligned once the electric current is applied to soil, which are otherwise in random state in the soil(Rhoades & Miyamoto, 1990).*1.3 SAR Backscatter coefficients*Backscatter is defined as the RADAR signal that returns to the receiver of the antenna after interaction with target under observation(Allbed & Kumar, 2013). The coefficient of scatter of RADAR signal in RADAR direction is called backscatter coefficient, represented by sigma nought σ^0(Verhoest et al., 2008). It is the RADAR backscatter per unit area of the distributed target with which the incident signal interacts. It is measured in degree decibels -dB

(Tripathi, Maithani & Kumar, 2018; Shashi, 2019; Tripathi & Maithani, 2018). Beta nought (β^0) is the brightness coefficient of the RADAR. It is a dimensionless quantity. Gamma nought (γ^0) is the RADAR backscatter coefficient dependent upon RADAR Brightness and incidence angle and is suitable for volume Scatterers(Saha, 2011; Tripathi and Tiwari, 2019).*1.4 Problem Statement*The prime objective of the study is to estimate the soil salinity in early stage of wheat crop growth at sub-surface level in a simple and robust way with freely available satellite datasets while maintaining the accuracy good enough.**2. Study Area and Datasets***2.1 Study Area*Rupnagar district of Punjab state in India is the study area for this study. Punjab has been the cradle of India's first green revolution and has been a primarily agriculture dependent state(Kumar, Kumar, & Mittal, 2004). Though in terms of annual rainfall, it lies in the semi-arid zone but owing to the nutrient rich alluvial soil brought down from the Himalayas by the five rivers and extensive canal and tube-well network for irrigation, Punjab leads the country in wheat production. Along with Haryana, it is the wheat bowl of the country. Rupnagar lies to the north of India's first planned city after independence-Chandigarh. Rupnagar is a district and headquarters of Rupnagar division of Punjab(Levinson et al., 2004). Rupnagar located on the banks of river Sutluj is one of the prominent sites of the erstwhile Indus Valley Civilization. Located between 30.97^0 N and 76.53^0 E, Rupnagar's average elevation is 260m above mean sea level and is bordered by the Shivalik hills of the mighty Himalayas in North and North-East(Kumar et al., 2004; Levinson et al., 2004).*2.2 Datasets*SAR/Microwave remote sensing data from Sentinel-1 satellite of the European Space Agency (ESA), Optical multispectral remote sensing data from Sentinel-2 satellite of the ESA. The datasets were acquired from the Alaska Satellite Facility (ASF) which is a freely available datasets for download from this portal. The data used were of 20^{th} November and 27^{th} December 2019 and 20^{th} January 2020, which were the days of satellite pass over Rupnagar. It was decided to acquire the field data of volumetric soil moisture and Electrical Conductivity (EC) simultaneously on the same dates at 60 cm depth. The following table (Table 2) gives details of Datasets used-**Table 2.** DATASETS USED

SL.No.	Data	Type	Spatial Resolution	Date of Acquisi
1.	Sentinel-1A	SAR/Microwave	20 m, Multilooked to 14 m	20/11/2019, 27/
2.	Sentinel-2A/B	Optical/Multi-spectral	10 m, resampled to 14 m	20/11/2019, 27/
3.	Field data	Electrical Conductivity, Volumetric Soil Moisture	————————	20/11/2019, 27/

Sentinel-1 is a microwave remote sensing satellite of the ESA that was launched in February 2014 as a part of ESA's Copernicus mission(Esch et al., 2019). It has an all-weather, all time data acquisition capacity. It operates in C-band with VV and VH polarizations. It has a 12-day repeat pass and has been used extensively for several applicable domains like crop and Land Use/Land Cover monitoring(Tripathi & Tiwari, 2019a). It has two different operation modes for land mass and over oceans to provide error and conflict free data acquisition(Crosetto et al., 2016). Main operational mode has 250km wide swath with a 20m spatial resolution at level-1 (L-1) product with high radiometric resolution(Shirvany, 2012). For this study Interferometric Wide Swath (IW) mode product, Single Look Complex (SLC) was chosen since it is the standard product over landmasses. The image was multilooked to 14m spatial resolution. There are three swaths of Terrain Observation with Progressive Scanning SAR (TOPSAR) in IW mode having a cross pass synchronization of burst for interferometric alignment. Sentinel-2 is an optical satellite of ESA's Copernicus program. Sentinel-2A (Calera et al., 2017) was launched in 2015 and 2B in 2017 with 7-year lifespan. It operates in 13 multispectral bands in visible, NIR and SWIR bands with 10-60m spatial resolutions. This study uses 10m resolution data from Sentinel-2B. The details of the study area are given in Figure 1 (Land Use/Land Cover map using Sentinel-1 SAR RGB image). -

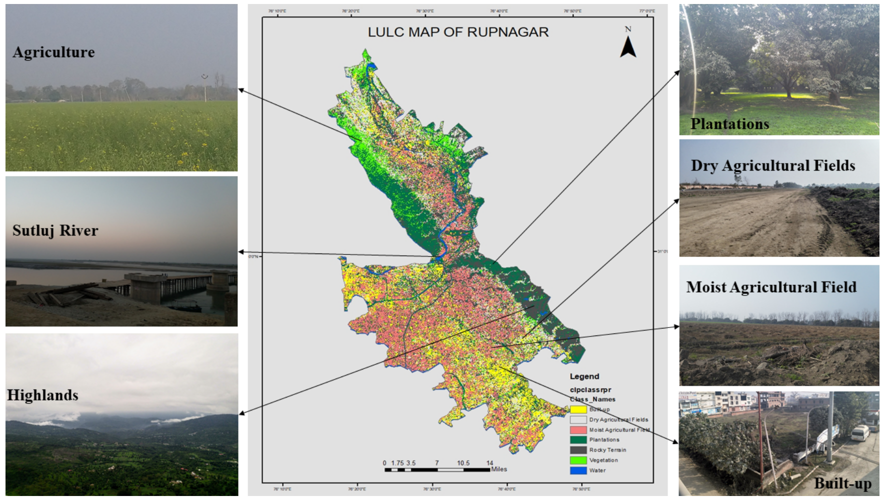

Figure.1. A classified Sentinel-1 SAR image showing Land Use/Land Cover details of study area- Rupnagar, Punjab

3. Methodology

Time series datasets, microwave data from Sentinel-1 and optical data from Sentinel-2 were taken. The microwave data was splitted. Calibrate and Deburst as a part of pre-processing. Thereafter the backscatter parameters σ^0, β^0 and γ^0 were retrieved during calibration. Thereafter, the data was geocoded using terrain correction from SRTM (Shuttle RADAR Topography Mission) plugin. Thereafter, the data was multilooked to generate square pixels and remove radiometric distortions.

The optical data of Sentinel-2, of the same dates as microwave data was taken and layer stacked to put together all 13 bands as a single imagery. Since the study area was not covered in one image tile, the different image tiles were mosaiced together. Thereafter, the study area of Rupnagar was clipped out from its district shape file. From the clipped imageries, band rationing was done to derive Normalised Differential Salinity Index (NDSI) which is an indicator of soil salinity from optical satellite data.

Since optical data does not have an all-weather availability and microwave data suffers from speckle noise, this study was aimed at retrieval of salinity sensitive parameters from both the datasets and put them together into one salinity estimation model. The model also uses field data collected using an instrument from FieldScout Ltd, USA. Surface Soil moisture, soil temperature and Electrical conductivity were recorded from this instrument at surface as well as at 60 cm below the surface in early stages of wheat crop growth (November 20th, 2019, December 27th, 2019, and January 20^{th,} 2020).

The SAR Backscatter coefficients, NDSI, surface soil moisture, soil electrical conductivity (EC) and soil temperature were fed into an Ordinary Least Squares Model. R^2 statistics, F-test and Durbin-Watson test were carried out to assess the model accuracy. The detailed methodology flow diagram is mentioned in Figure 2.

Prior to model development, correlative plots were made to check the sensitivities of all other parameters used in the model with the most indicative of Soil Salinity – EC and NDSI. Also, the three backscatter parameters were plotted for correlation with Sigma Nought σ^0 for any major variation since use of excess parameters could lead to model overfitting.

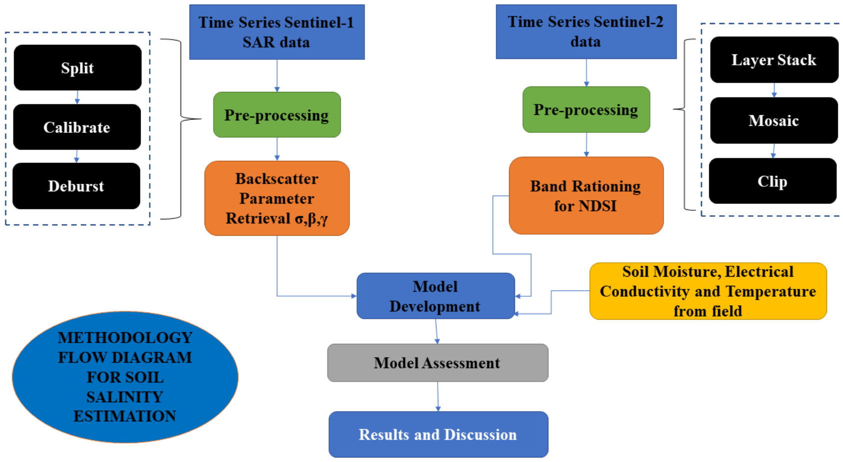

Figure.2. Methodology Flow Diagram

3.1 Band Rationing for NDSI

From the clipped image of Rupnagar, the salinity sensitive bands were used for generation of NDSI. The NDSI values range from -1 to1 with 1 representing high salinity values in soil(Konukcu et al., 2006). Studies reveal that the Red and NIR bands are the most sensitive to the soil ions causing salinity(Rengasamy et al., 2003). The following formula was used for the purpose-

NDSI=$\frac{(Green-SWIR)}{(Green+SWIR)}$ (1)

Since the bands 3 (GREEN) and Band 11 (Short Wave InfraRed-SWIR) have spatial resolutions of 10 m and 20 m respectively, the optical image bands were resampled at 14 m spatial resolution (same as that of multilooked Sentinel-1 SAR image). Based on this, surface Salinity maps for entire Rupnagar district were generated for the study dates of 4th December and 27th December 2019 and 20th January 2020. The application of fertilizers mainly DDT (Dichlorodiphenyltrichloroethane) affected the salinity levels, declining between the first two dates of early stage of wheat crop growth to slightly rising in January. The details are shown in the maps in Figure 3-

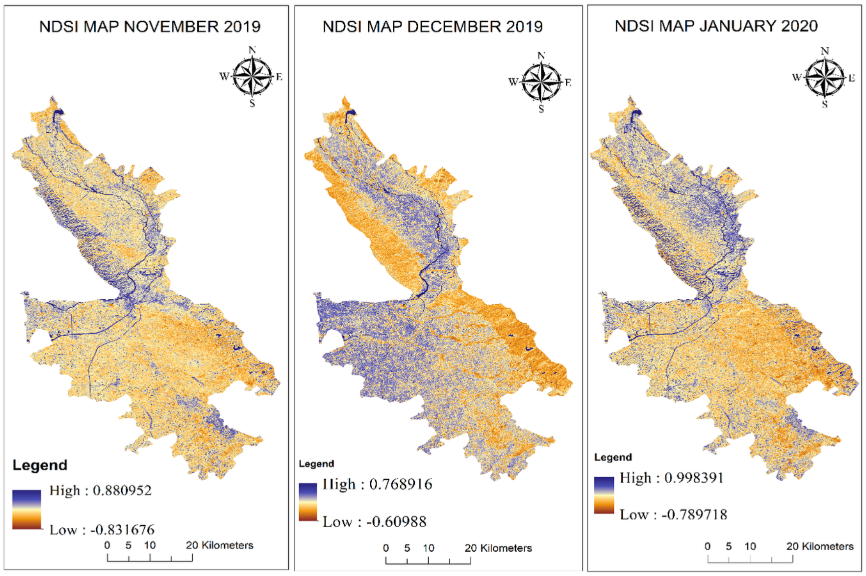

Figure 3. NDSI Maps generated from Sentinel-2 Optical Multi-spectral data for – (A) 20TH November 2019, (B) 27TH December 2019 and, (C) 20THJanuary 2020

The maximum values of NDSI for first two dates were 0.78 and 0.87 respectively while after the application of fertilisers in January first week (as told by the local farmers), there was an increase in salinity levels and maximum value increased to 0.973.

3.2 Correlations of Parameters with EC at 60 cm depth

The various backscatter parameters were analysed for correlation with Electrical Conductivity (EC) and NDSI for both VH and VV polarisation channels. For σ^0, β^0 and γ^0, high values of R^2 statistics for correlation were given as shown in Figures 4. Figure 4 shows the correlative plots for σ^0in VH and VV polarisation with Surface EC for all three dates, since C-band SAR waves are affected by the surface soil conditions and interacts with the surface soil ions as shown by Figure 4-

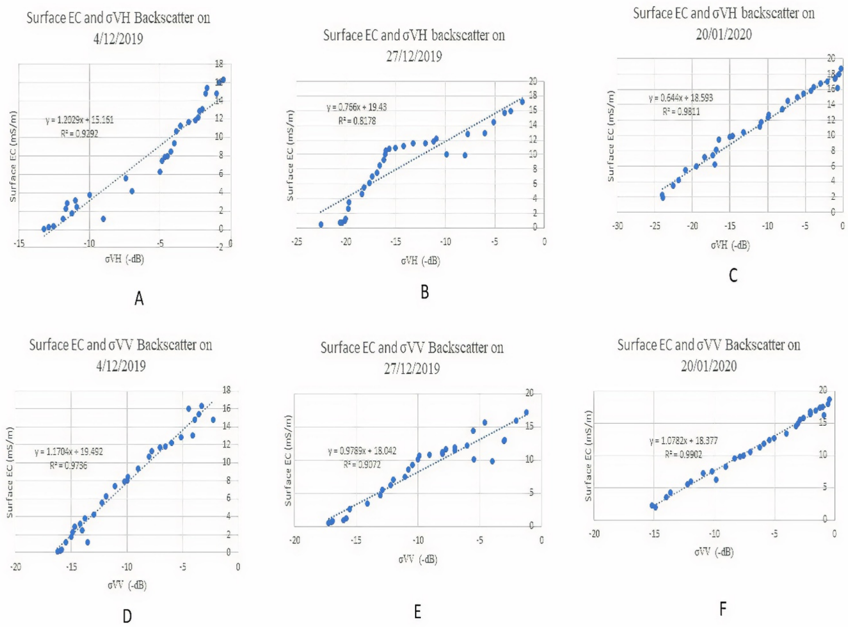

Figure.4. Correlative plots for Surface Electrical Conductivity and VH backscatter (A to C) and VV polarization backscatter (D to F)

since SAR waves interact with the surface, but it's the root zone soil salinity that affects the plant growth hence its important to establish a correlation between surface soil salinity that interacts with the RADAR waves and the root zone soil salinity. This is done to establish an indirect relation between RADAR backscatter and root zone electrical conductivity (which is indicative of soil salinity). So that, satellite data could be used for modelling and estimation of soil salinity in root zone.

Figure 5, shows the correlative relation between surface EC and root zone EC.

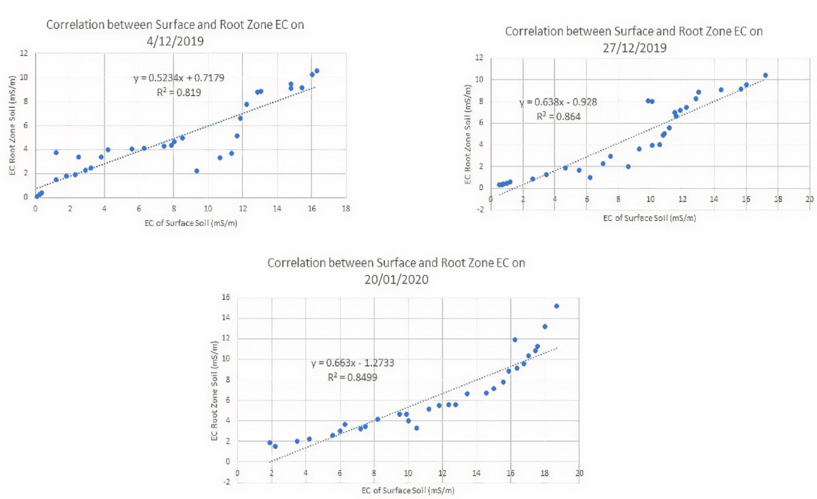

Figure 5. Correlation between surface EC and sub-surface (60 cm depth) soil EC for 4th December 2019,

27^{th}December 2019, and 20^{th} January 2020.

The surface parameters from field were found to directly correlate to the satellite data parameters of SAR backscatter and NDSI, hence an attempt was made to correlate the satellite data parameters with sub-surface field parameters which showed high correlation as shown in Figures 4 and 5 above. Hence, sub-surface soil moisture and EC values were used for regression analysis along with satellite data. 60 cm depth was chosen since in early stage of wheat crop growth, this is the root zone depth of wheat crop.

3.3 Calibration

Calibration is done to relate the pixel values directly with the backscatter thus quantifying the SAR image(Ballester-berman, Lopez-sanchez, & Fortuny-guasch, 2005; Hari Shanker Srivastava et al., 2008). Calibration vector on addition as an annotation product facilitates the conversion of backscatter values of intensity into the different backscatter coefficient values of σ^0, radar brightness coefficient β^0 and volumetric scatter coefficient γ^0(Boerner, 2012; Hsieh et al., 2011)·

Where,

$\beta^0 = k \times DN^2$ (2)

where β^0 is RADAR brightness coefficient, k is calibration coefficient that relates the Backscatter to pixel values using simple mathematical formula and in turn provides radiometric correction to the imagery(Srivastava et al., 2009).

$\sigma^0 = \beta^0 \times \sin\,(i_{x,y})$ (3)

Where σ^0 is RADAR backscatter coefficient expressed in degree decibels (-dB). And $i_{x,y}$ is local incidence angle at which the RADAR waves interact with the target(Tiwari, 2019; Veci, 2016).

$\gamma^0 = \beta^0 \times \tan\,(i_{x,y})$ (4)

where, γ^0 is the backscatter coefficient for volumetric Scatterers.

Calibration replaces the sensor level scaling of the imagery with user defined scaling. The Sentinel-1, L-1 products provide four Look Up Tables (LUTs) corresponding to the four backscatter coefficients and their Digital Number (DN) values(Zhou, Pan, Zhang, Wei, & Han, 2017).

The LUTs apply a gain depending upon the absolute calibration constant. The following formula applies radiometric calibration(Tapete, Cigna, & Donoghue, 2016)-

Values (i) $= \frac{|DN|^2}{Ai^2}$ (5)

Where Values (i) = anyone of the backscatter coefficients or their DN values and A_i = one of β_i, σ_i

3.4 Deburst

The Terrain Observation with Progressive Scanning SAR (TOPSAR) in IW mode product acquires single image per swath per polarization mode(Keydel, 2007). Each IW product has three swath and acquisition is done in sub-swaths with successive burst series(Tripathi, Kumar, & Maithani, 2018). This step is used to compensate for the pixel spacings in both range and azimuth direction for better acquisition and sub-swath synchronisation(Hoa et al., 2019).

3.5 Multilooking

Due to different spatial resolutions in range and azimuth directions, speckle noise adds up and leads to a lot of speckle in the imagery(Fawwaz T. Ulaby, F. Kouyate & Williams, 1986). To overcome this noise and generate square pixels, multilooking is carried out. In this study 14.15m was the resultant spatial resolution of the multilooked image(Yang et al., 2011).

3.6 Terrain Correction

Since, the topography varies with the sensor tilt, there is an inherent distortion in the imagery(Baghdadi et al., 2012). The far-off features from the nadir appear more distorted. To overcome this distortion and relate the image co-ordinates to the actual ground co-ordinates, terrain correction is done.

3.7 Model Development

Ordinary Least Squares (OLS) regression was used for modelling and estimation of soil salinity. The parameters chosen were soil moisture, soil temperature and root zone electrical conductivity from field and RADAR backscatter for VH and VV polarisations, NDSI from optical Sentinel -2 data.

The OLS model is robust for estimation of parameters that are unknown in a linear regression model. The OLS is a type of multiple linear regression model and is expressed as(Ferreyra, Curci, & Lanfri, 2016)-

$\mathrm{Y_n} = \sum_{i=0}^{k} \beta_\mathrm{i} \mathrm{x_{ni}} + \varepsilon_\mathrm{n}$ (6)

And $\mathrm{Y_i} = \beta_0 + \beta_1 \mathrm{x_i} + \varepsilon_\mathrm{i}$(7)

Where, $\mathrm{Y_i}$ is the dependent variable whereas, β_0 is intercept of y and β_1 is coefficient of slope and ε_i is term denoting random error(Reynolds et al., 2018).

It was aimed to ascertain the dependency of various parameters since an OLS model performs better with more than one predictor, on the soil salinity in root zone that affects the crop growth. The model did not use RADAR brightness term and volume Scatterers since they had high dependence on each other and Had nearly equal values. Using them would lead to overfitting the model giving exceptionally high values of R^2-statistics in training phase. Thirty -two different locations in various agricultural zones of Rupnagar district were chosen to collect field data for the three dates as mentioned earlier. The RADAR backscatter values for the same locations were used in the model. The model is as follows-

$$\text{Soil\_Salinity} = \beta 0 + \beta 1 \times \sigma \text{VH} + \beta 2 \times \sigma \text{VV} + \beta 3 \times Soil\ Moisture + \beta 4 \times NDSI + \beta 5 \times EC\text{ROOT ZONE} + \beta 6 \times Temperature\ in\ F \quad (8)$$

Where, β0, β1.... β5 are all regression coefficients, NDSI is Normalized Differential Soil Salinity Index, EC is electrical conductivity in milli siemens per centimetre and σ_{VH} and σ_{VV} are backscatter coefficients for VH and VV polarization channels.

Field data collection for soil electrical conductivity and soil moisture was collected from an instrument of field Scout USA which was well calibrated in distilled water (EC=0 mS/cm) and thermal data was collected from thermal imaging camera sensor from Seek Thermal. The field photographs are shown in Figure 6-

Figure 6. Data Collection from Agriculture Field

4. Results and Discussion

The Ordinary Least Squares (OLS) regression was used for modelling and prediction of soil salinity in the root zone. Data from first two dates (4th and 27th December 2019) with all parameters was used to train the model while validation was done using the data of 20th January 2020. A correlation heat map shown in Figure 7, shows the correlation between the different parameters used for modelling. It also shows the strong correlation between different satellite and on ground sensor parameters with soil salinity indicators of EC and NDSI-

Hosted file

`image7.emf` available at https://authorea.com/users/354002/articles/477698-a-simplified-sub-surface-soil-salinity-estimation-using-synergy-of-sentinel-1-sar-and-sentinel-2-multispectral-satellite-data-for-early-stages-of-wheat-crop-growth-in-rupnagar-punjab-india

Figure 7. Correlation Heat Map

The OLS model gave high R^2-statistics in testing and training phases, respectively. The R^2-statistics in training was 0.997 and in testing 0.958 which means 99.7% and 95.8% accuracies at respective stages. The results are shown in Figure 8-

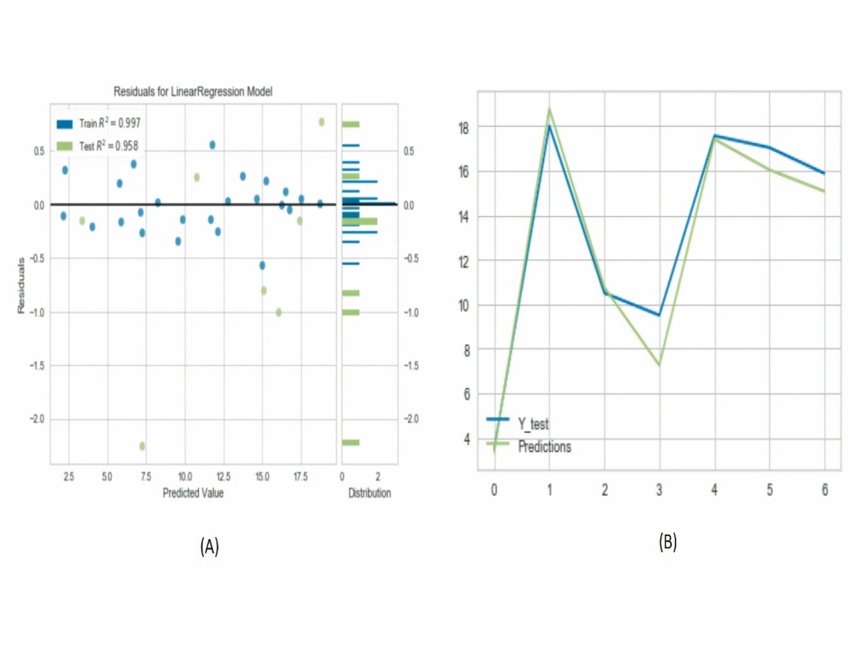

Figure. 8. (A) R^2-statistics in testing and training phases, (B) Goodness of Fit

4.1 Accuracy Assessment

4.1.1 The F-test

An F-test was conducted to cross check the model accuracy and goodness of fit, since the R^2-statistic only gives the variation of dependent variable with the independent variable(Forest et al., 2001). The adjusted R^2 tests the results based on independent variables only. The F-test statistic is indicative of response and predictor relation. A low F value means a weak relation and a zero F value would mean there is no relationship at all(Loureiro & González, 2008).

The higher the F-value more than 1 gives enough reason to reject the null hypothesis (H_0) that all regression coefficients are zero (β$_0$, β$_1$, β$_2$, β$_3$. . . . . . βn =0). An F-test statistic is calculated by(Forest et al., 2001; Loureiro & González, 2008)-

F=$\frac{(TSS-RSS)/p}{RSS/(n-p-1)}$ (9)

Where TSS is total sum of squares, TSS= Σ (?$_?$ - (y)^2 and RSS is the Residual Sum of Squares RSS= Σ (?$_?$ - ($\hat{y}$))^2 , and y_i is response value, $\hat{y}$ is predicted value and$y$ is sample mean(Happé & Frith, 2006).

The OLS regression results are given in TABLE 3 at 97.5% confidence level-

TABLE 3. OLS Regression Residuals

Coefficient	**Strd. Error**
0.1726	0.295
-0.7872	0.122
0.0222	0.392
-0.0720	0.070
-0.3572	0.911
0.6151	0.308

Coefficient	**Strd. Error**
0.2075 0.1819 -0.0184 0.1373 2.3494 -0.2951 0.0719 0.8728 -0.0213 0.0459	0.221 0.259 0.103 0.121 1.923 0.925 0.258 0.368 0

The F-test value was 1686 which was well above zero and gave compelling evidence to reject the null hypothesis (H_0). The adjusted R^2 value was 0.98. The standard error value from the above table is below 0.5 for most cases which gives information of standard deviation of coefficients and their variations. The P-value shows that each variable has some correlation with independent variables at 97.5% level of confidence.

4.1.2 Durbin-Watson test

The Durbin-Watson test is conducted in statistics to check for autocorrelation existing between the residuals in a linear regression analysis(Chen, 2016). A positive autocorrelation value between 0 to 2 means that the model fits properly(Hepple, 1998). A value less than 0 and more than 2.5 is a cause for concern as it would mean too much of outliers in the data or model overfitting. In this study, the Durbin Watson value was found to be 1.65 which shows that model fits well and accurately(Chen, 2016; Happé & Frith, 2006; Hepple, 1998).

4.2 Discussion

The results show that for soil which has a horizontal expanse over vast areas VH polarization is the obvious choice for modelling, but it gets attenuated when the soil texture is rough and there is sprouting of crop. Hence a combination of both VV and VH backscatter parameters from SAR satellite data were used for modelling. For soil salinity indices development from Sentinel-2 data, Band 3 (Green) and Band 11 (Short Wave InfraRed- SWIR) were used since saline soils reflect more in Green to SWIR Bands. Hence NDSI generated was (refer to Section 3.1) used as another parameter. The other parameters came from field data such as temperature, soil moisture and soil electrical conductivity for surface as well as root zone. Since satellite data is indicative of only surface phenomenon hence a correlation was established between surface parameters from field and root zone parameters. Thereafter, a correlation was established between satellite and root zone parameters collected from field by digging up to 2 ft (0.6 m) depth since crop roots do not extent any further beyond. The Root zone parameters were then used for modelling since all the above-mentioned correlative plots gave an average R^2-statistics in correlation above 0.8 (80%). The model gave highly accurate results in the limited resources available with two polarization channels of SAR data and no complex modelling approach and sophisticated chemical lab tests.

The estimated sub-surface soil salinity map in terms of Electrical Conductivity for Rupnagar is shown in Figure 9-

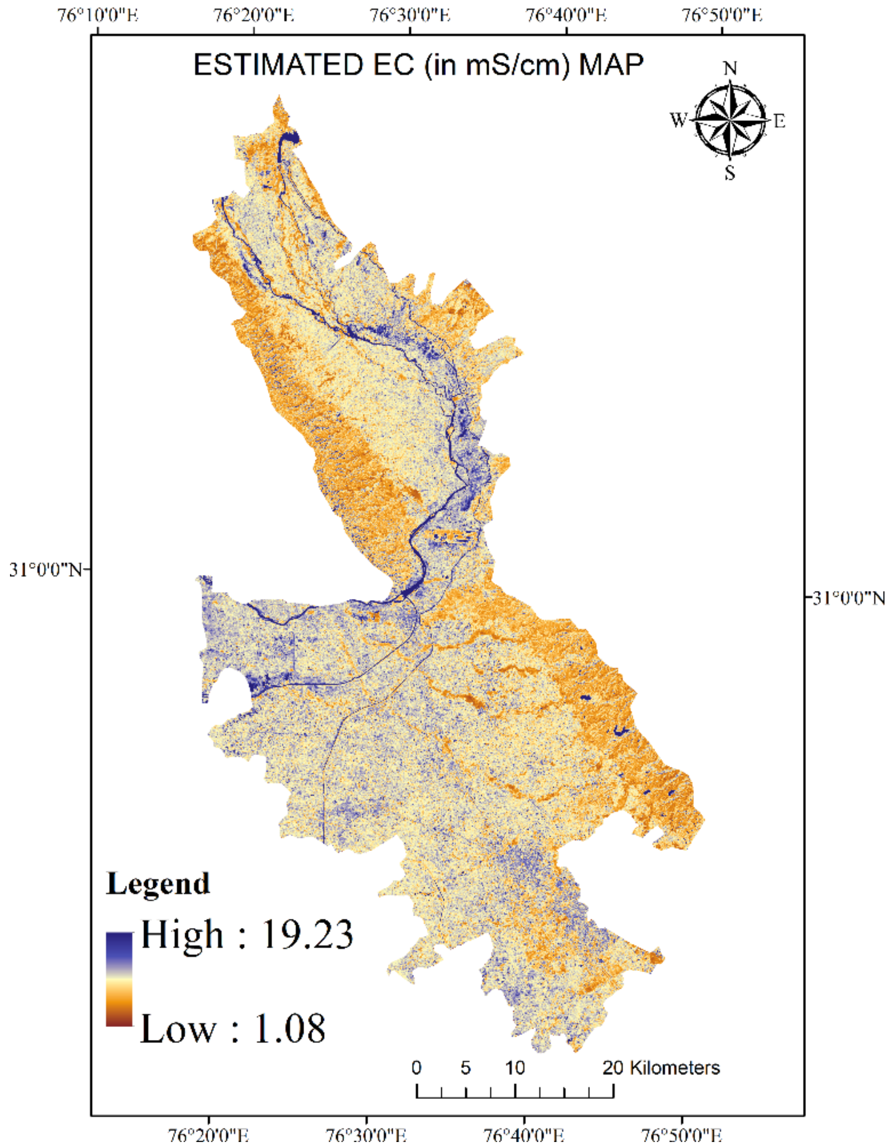

Figure 9. Estimated Sub-Surface Electrical Conductivity (EC) Map for January 2020 of Rupnagar

5. Conclusion(s)

The results (Refer to section 4) show that dual polarized SAR data along with optical multispectral data if used in a synergetic way by taking the advantages of both in terms of parameters that can be derived from them can be used in a simple modelling approach for Root Zone soil salinity estimation. Till now, most soil salinity studies were concentrated only upon the surface soil salinity despite using highly advanced datasets which were costly and sophisticated laboratory tests of soil samples. This study not only conducted in a highly cost-effective manner but also aimed at a simple, robust, and accurate approach. The results show that the study has been highly accurate with high values of R^2-statistics of 0.997 and 0.958 in training and testing stages, respectively. The accuracy and goodness of model fit was further strengthened by the F-test and DW tests as mentioned in results section. The novelties from this study are that this study is innovative in a manner that it uses Microwave and Optical data from satellites, thermal data from thermal imaging sensor from field thus giving it a multi sensor approach for soil salinity estimation at sub-surface level with high accuracy with a simple approach. The study made use of freely available Sentinel-1 SAR and Sentinel-2 optical satellite data, and no sophisticated laboratory analysis hence making it cost-effective and time saving. The study estimates root zone soil salinity from satellite data unlike most other studies which were confined to surface soil salinity estimation using remote sensing.

The study establishes a fact that remote sensing could be used effectively and accurately for root zone soil salinity estimation which is a major cause of crop failure and low yields world-wide. The findings could be used for planning and taking timely measures for soil health enhancement.

As an improvement and future extension to the work, a longer time series SAR dataset could be utilised at higher wavelengths (L and S band) at monthly intervals and soil salinity variations can be studied with crop growth monitoring simultaneously. At present, the study has been conducted for Rupnagar district of Punjab. Further the technique is being implemented for other areas in India and is expected to deliver similar results.

Acknowledgements

The authors express their gratitude to the Department of Civil Engineering, Indian Institute of Technology (IIT) Ropar, Rupnagar (Punjab), India for technical support and Dr. Dara Entekhabi, Professor- Bacardi and Stockholm Water Foundations Professor in the Department of Civil and Environmental Engineering and the Department of Earth, Atmospheric and Planetary Sciences at Massachusetts Institute of Technology (USA) and Science Team Leader of NASA SMAP (Soil Moisture Active Passive) mission, for his valuable appreciation towards developing the final form of this study.

Conflict of Interest

The authors declare no conflict of Interest.

Data Availability Statement

The data that support the findings of this study are available from the corresponding author upon reasonable request.

References

Ahmed, E., & Luis, G. (2010). Comparison of Ordinary Kriging, Regression Kriging, and Cokriging Techniques to Estimate Soil Salinity Using LANDSAT Images. *Journal of Irrigation and Drainage Engineering* , *136* (6), 355–364. https://doi.org/10.1061/(ASCE)IR.1943-4774.0000208

Akshar Tripathi, Sandeep Maithani, S. K. (2018). Minimization of the Ambiguity of Merging of Urban Builtup and Fallow land Features by Generating ‘ C2 ’ Covariance Matrix using Spaceborne Bistatic Dual Pol SAR Data. *IEEE XPLORE* , (March). https://doi.org/10.1109/RAIT.2018.8389058

Allbed, A., & Kumar, L. (2013). Soil Salinity Mapping and Monitoring in Arid and Semi-Arid Regions Using Remote Sensing Technology: A Review.*Advances in Remote Sensing* , *02* (04), 373–385. https://doi.org/10.4236/ars.2013.24040

Amin, A. A. (2004). The extent of desertification on Saudi Arabia.*Environmental Geology* , *46* (1), 22–31. https://doi.org/10.1007/s00254-004-1009-0

Anderson, K., & Croft, H. (2009). Remote sensing of soil surface properties. *Progress in Physical Geography 33(4) (2009) Pp. 457–473* , *33* (4), 457–473. https://doi.org/10.1177/0309133309346644

Arora, N. K., Fatima, T., Mishra, I., Verma, M., Mishra, J., & Mishra, V. (2018). Environmental sustainability: challenges and viable solutions. *Environmental Sustainability* , *1* (4), 309–340. https://doi.org/10.1007/s42398-018-00038-w

Aslan, A., Rahman, A. F., Warren, M. W., & Robeson, S. M. (2016). Remote Sensing of Environment Mapping spatial distribution and biomass of coastal wetland vegetation in Indonesian Papua by combining active and passive remotely sensed data. *Remote Sensing of Environment* ,*183* , 65–81. https://doi.org/10.1016/j.rse.2016.04.026

Baghdadi, N., Cresson, R., Pottier, E., Aubert, M., Mehrez, Z., & Jacome, A. (2012). A potential use for the C-band polarimetric SAR parameters to characterise the soil surface over bare agriculture fields, (January 2011). https://doi.org/10.1109/TGRS.2012.2185934

Baig, M. B., & Shahid, S. A. (2014). Managing Degraded Lands for Realizing Sustainable Agriculture Through Environmental Friendly Technologies BT - Science, Policy and Politics of Modern Agricultural System: Global Context to Local Dynamics of Sustainable Agriculture. In M. Behnassi, S. A. Shahid, & N. Mintz-Habib (Eds.) (pp. 141–164). Dordrecht: Springer Netherlands. https://doi.org/10.1007/978-94-007-7957-0_10

Ballester-berman, J. D., Lopez-sanchez, J. M., & Fortuny-guasch, J. (2005). Retrieval of Biophysical Parameters of Agricultural Crops Using Polarimetric SAR Interferometry, *43* (4), 683–694.

Bhutta, M. N., & Smedema, L. K. (2007). One hundred years of waterlogging and salinity control in the Indus valley, Pakistan: a historical review. *Irrigation and Drainage* , *56* (S1), S81–S90. https://doi.org/10.1002/ird.333

Boerner, W. M. (2012). Implementation of FULL-POL-SAR in agriculture, forestry and aquaculture as well as for the detection of natural hazards plus natural disaster assessment from air and space in South, East and Pacific Asia. *EUSAR 2012; 9th European Conference on Synthetic Aperture Radar* .

Braidwood, R. J. (1960). The Agricultural Revolution Author (s): Robert J . Braidwood Source : Scientific American , Vol . 203 , No . 3 (September 1960), pp . 130-152 Published by : Scientific American , a division of Nature America , Inc . Stable URL : https://www.jstor.org/,*203* (3), 130–152. Retrieved from https://www.jstor.org/stable/pdf/24940620.pdf

Calera, A., Campos, I., Osann, A., Urso, G. D., & Menenti, M. (2017). Remote Sensing for Crop Water Management : From ET Modelling to Services for the End Users. *Sensors, MDPI* , 1–25. https://doi.org/10.3390/s17051104

Calvão, T., & Palmeirim, J. M. (2004). Mapping Mediterranean scrub with satellite imagery: biomass estimation and spectral behaviour.*International Journal of Remote Sensing* , *25* (16), 3113–3126. https://doi.org/10.1080/01431160310001654978

Cassman, K. G., Dobermann, A., Walters, D. T., & Yang, H. (2003). Meeting Cereal Demand While Protecting Natural Resources and Improving Environmental Quality. *Annual Review of Environment and Resources* , *28* (1), 315–358. https://doi.org/10.1146/annurev.energy.28.040202.122858

Chen, Y. (2016). Spatial Autocorrelation Approaches to Testing Residuals from Least Squares Regression. *PloS One* , *11* (1), e0146865–e0146865. https://doi.org/10.1371/journal.pone.0146865

Chong, I., & T, C. J. (2005). Performance of some variable selection methods when multicollinearity is present. *Chemometrics and Intelligent Laboratory Systems* , *78* , 103–112. https://doi.org/10.1016/j.chemolab.2004.12.011

Congalton, R. G., Fenstermaker, L., & Mcgwire, K. C. (1991). Remote sensing and geographic information system data integration : error sources and research issues. *American Society for Photogrammetry and Remote Sensing* , (January). Retrieved from https://www.researchgate.net/profile/Lynn_Fenstermaker/publication/238307070_Remote_sensing_and_geographic_information_system_data_integration_error_sources_and_research_issues/links/0f31753b466ff6c507000000.pdf

Corwin, D. L., & Lesch, S. M. (2003). Application of Soil Electrical Conductivity to Precision Agriculture. *Agronomy Journal* ,*95* (3), 455–471. https://doi.org/10.2134/agronj2003.4550

Corwin, D. L., & Lesch, S. M. (2005). Apparent soil electrical conductivity measurements in agriculture. *Computers and Electronics in Agriculture* , *46* , 11–43. https://doi.org/10.1016/j.compag.2004.10.005

Crosetto, M., Monserrat, O., Cuevas-Gonzalez, M., Devanthery, N., & Crippa, B. (2016). Persistent Scatterer Interferometry: A review.*ISPRS Journal of Photogrammetry and Remote Sensing* , *115* , 78–89. https://doi.org/10.1016/j.isprsjprs.2015.10.011

David R . Anderson, K. P. . B. and W. L. . T. (2000). Null Hypothesis Testing : Problems , Prevalence , and an Alternative. *Wiley* ,*64* (4), 912–923. https://doi.org/10.2307/3803199

Davidson, N. C., & Finlayson, C. M. (2007). Earth Observation for wetland inventory , assessment and monitoring. *AQUATIC CONSERVATION: MARINE AND FRESHWATER ECOSYSTEMS* , *228* , 219–228. https://doi.org/10.1002/aqc

Dekker, R. J. (1998). Speckle filtering in satellite SAR change detection imagery. *International Journal of Remote Sensing* ,*19* (6), 1133–1146. https://doi.org/10.1080/014311698215649

Delaney, H. and. (1974). Dielectric Properties of Soils at UHF and Microwave Frequencies. *JOURNAL OF GEOPHYSICAL RESEARCH* ,*79* (11). https://doi.org/https://doi.org/10.1029/JB079i011p01699

Dumanski Samuel Pieri, Christian Agriculture and Agri-Food Canada, J. G. (1998). *Indicators of land quality and sustainable land management* . The World Bank. https://doi.org/doi:10.1596/0-8213-4208-8

Egamberdieva, D., Li, L., Lindstrom, K., & Rasanen, L. A. (2016). A synergistic interaction between salt-tolerant Pseudomonas and Mesorhizobium strains improves growth and symbiotic performance of liquorice (Glycyrrhiza uralensis Fish.) under salt stress. *Applied Microbiology and Biotechnology* , *100* (6), 2829–2841. https://doi.org/10.1007/s00253-015-7147-3

Engman, E. T. (1991). Applications of Microwave Remote Sensing of Soil Moisture for Water Resources and Agriculture. *Remote Sensing of Environment* , *226* , 213–226. https://doi.org/https://doi.org/10.1016/0034-4257(91)90013-V

Esch, S., Reichenau, T. G., Schneider, K., Esch, S., Korres, W., Reichenau, Schneider, K. (2019). Soil moisture index from ERS-SAR and its application to the analysis of spatial patterns in agricultural areas the analysis of spatial patterns in agricultural areas,*12* (2). https://doi.org/10.1117/1.JRS.12.022206

Etehadnia, M., Waterer, D., De Jong, H., & Tanino, K. K. (2008). Scion and Rootstock Effects on ABA-mediated Plant Growth Regulation and Salt Tolerance of Acclimated and Unacclimated Potato Genotypes. *Journal of Plant Growth Regulation* , *27* (2), 125–140. https://doi.org/10.1007/s00344-008-9039-6

Fawwaz T. Ulaby, F. Kouyate, B. B., & Williams, A. T. H. L. (1986). Textural Information in SAR Images. *IEEE TRANSACTIONS ON GEOSCIENCE AND REMOTE SENSING, VOL. GE-24, NO. 2, MARCH 1986* , (2), 235–245. https://doi.org/10.1109/TGRS.1986.289643

Ferreyra, M. F. G., Curci, G., & Lanfri, M. (2016). First Implementation of the WRF-CHIMERE-EDGAR Modeling System Over Argentina.*IEEE Journal of Selected Topics in Applied Earth Observations and Remote Sensing* . https://doi.org/10.1109/JSTARS.2016.2588502

Forest, C. E., Allen, M. R., Sokolov, A. P., & Stone, P. H. (2001). Constraining climate model properties using optimal fingerprint detection methods. *Climate Dynamics* , *18* (3), 277–295. https://doi.org/10.1007/s003820100175

Frackowiak, E. (2001). Carbon materials for the electrochemical storage of energy in capacitors. *Carbon* , *39* , 937–950. https://doi.org/https://doi.org/10.1016/S0008-6223(00)00183-4

Franzini, V. I., Azcon, R., Ruiz-Lozano, J. M., & Aroca, R. (2019). Rhizobial symbiosis modifies root hydraulic properties in bean plants under non-stressed and salinity-stressed conditions. *Planta* ,*249* (4), 1207–1215. https://doi.org/10.1007/s00425-018-03076-0

Garcia-Tejero, I. F., Duran-Zuazo, V. H., Muriel-Fernandez, J. L., & Rodriguez-Pleguezuelo, C. R. (2011). Water and Sustainable Agriculture BT - Water and Sustainable Agriculture. In I. F. Garcia-Tejero, V. H. Duran-Zuazo, J. L. Muriel-Fernandez, & C. R. Rodriguez-Pleguezuelo (Eds.) (pp. 1–94). Dordrecht: Springer Netherlands. https://doi.org/10.1007/978-94-007-2091-6_1

Guzha, A. C. (2004). Effects of tillage on soil microrelief , surface depression storage and soil water storage. *Soil Tillage and Research* , *76* , 105–114. https://doi.org/10.1016/j.still.2003.09.002

HANSEN, M., DUBAYAH, R., & DEFRIES, R. (1996). Classification trees: an alternative to traditional land cover classifiers. *International Journal of Remote Sensing* , *17* (5), 1075–1081. https://doi.org/10.1080/01431169608949069

Happe, F., & Frith, U. (2006). The Weak Coherence Account: Detail-focused Cognitive Style in Autism Spectrum Disorders.*Journal of Autism and Developmental Disorders* , *36* (1), 5–25. https://doi.org/10.1007/s10803-005-0039-0

Hepple, L. W. (1998). Exact Testing for Spatial Autocorrelation among Regression Residuals. *Environment and Planning A: Economy and Space* , *30* (1), 85–108. https://doi.org/10.1068/a300085

Herrick, J. E. (2000). Soil quality : an indicator of sustainable land management ? *Applied Soil Ecology* , *15* , 75–83. https://doi.org/https://sci-hub.tw/10.1016/S0929-1393(00)00073-1

Hoa, P., Nguyen Vu, G., Nguyen, B., Le, H., Pham, T. D., Hasanlou, M., & Tien Bui, D. (2019). *Soil Salinity Mapping Using SAR Sentinel-1 Data and Advanced Machine Learning Algorithms: A Case Study at Ben Tre Province of the Mekong River Delta (Vietnam)* . *Remote Sensing* . https://doi.org/10.3390/rs11020128

Holmes, R. M. (1959). A modulated soil moisture budget. *Monthly Weather Review* , (March), 101–105. Retrieved from http://citeseerx.ist.psu.edu/viewdoc/download?doi=10.1.1.395.2341&rep=rep1&type=pdf

Hong, S., & Pan, H. (2000). Impact of soil moisture anomalies on seasonal , summertime circulation over North America in a Regional Climate Model, *105* , 625–634. https://doi.org/https://doi.org/10.1029/2000JD900276

Hsieh, C. S., Shih, T. Y., Hu, J. C., Tung, H., Huang, M. H., & Angelier, J. (2011). Using differential SAR interferometry to map land subsidence: A case study in the Pingtung Plain of SW Taiwan.*Natural Hazards* , *58* (3), 1311–1332. https://doi.org/10.1007/s11069-011-9734-7

Hu, Y., & Schmidhalter, U. (2005). Drought and salinity: A comparison of their effects on mineral nutrition of plants. *Journal of Plant Nutrition and Soil Science* , *168* (4), 541–549. https://doi.org/10.1002/jpln.200420516

Igartua, E., Gracia, M. P., & Lasa, J. M. (1994). Characterization and genetic control of germination-emergence responses of grain sorghum to salinity. *Euphytica* , *76* (3), 185–193. https://doi.org/10.1007/BF00022163

Jolly, I. D., McEwan, K. L., & Holland, K. L. (2008). A review of groundwater–surface water interactions in arid/semi-arid wetlands and the consequences of salinity for wetland ecology. *Ecohydrology* ,*1* (1), 43–58. https://doi.org/10.1002/eco.6

Jordan, M. M., Navarro-Pedreno, J., Garcia-Sanchez, E., Mateu, J., & Juan, P. (2004). Spatial dynamics of soil salinity under arid and semi-arid conditions: geological and environmental implications.*Environmental Geology* , *45* (4), 448–456. https://doi.org/10.1007/s00254-003-0894-y

Katsaros, K. B., Vachon, P. W., Liu, W. T., & Black, P. G. (2002). Microwave Remote Sensing of Tropical Cyclones from Space. *Journal of Oceanography* , *58* (1), 137–151. https://doi.org/10.1023/A:1015884903180

Keydel, W. (2007). Normal and Differential SAR Interferometry.*Radar Polarimetry and Interferometry* , (October), 3-1-3–36. Retrieved from http://www.dtic.mil/cgi-bin/GetTRDoc?Location=U2&doc=GetTRDoc.pdf&AD=ADA470882

Kim, J.-E., & Hong, S.-Y. (2007). Impact of Soil Moisture Anomalies on Summer Rainfall over East Asia: A Regional Climate Model Study. *Journal of Climate* , *20* (23), 5732–5743. https://doi.org/10.1175/2006JCLI1358.1

Koevoets, I. T., Venema, J. H., Elzenga, J. T. M., & Testerink, C. (2016). Roots Withstanding their Environment: Exploiting Root System Architecture Responses to Abiotic Stress to Improve Crop Tolerance . *Frontiers in Plant Science* . Retrieved from https://www.frontiersin.org/article/10.3389/fpls.2016.01335

Konukcu, F., Gowing, J. W., & Rose, D. A. (2006). Dry drainage : A sustainable solution to waterlogging and salinity problems in irrigation areas ? *Agricultural Water Management* , *83* , 1–12. https://doi.org/10.1016/j.agwat.2005.09.003

Kumar, P., Kumar, A., & Mittal, S. (2004). Total Factor Productivity of Crop Sector in the Indo-Gangetic Plain of India: Sustainability issues revisited. *Indian Economic Review* , *39* (1), 169–201. Retrieved from http://www.jstor.org/stable/29793810

Landauer, R. (1978). Electrical conductivity in inhomogeneous media. *AIP Conference Proceedings* , *40* (1), 2–45. https://doi.org/10.1063/1.31150

Larson, K. M., Braun, J. J., Small, E. E., Zavorotny, V. U., Gutmann, E. D., & Bilich, A. L. (2010). GPS Multipath and Its Relation to Near-Surface Soil Moisture Content. *IEEE Journal of Selected Topics in Applied Earth Observations and Remote Sensing* , *3* (1), 91–99. https://doi.org/10.1109/JSTARS.2009.2033612

Leckie, D. G. (1984). Advances in remote sensing technologies for forest surveys and management. *Canadian Journal of Forest Research* . https://doi.org/https://doi.org/10.1139/x90-063

Levinson, F. J., Mehra, S., Levinson, D., Chauhan, A. K., Koppe, G., Bence, B., & Almedom, A. M. (2004). Morinda Revisited: Changes in Nutritional Well-Being and Gender Differences after 30 Years of Rapid Economic Growth in Rural Punjab, India. *Food and Nutrition Bulletin* , *25* (3), 221–227. https://doi.org/10.1177/156482650402500301

Lewis, S. L., & Maslin, M. A. (2015). Defining the Anthropocene. *Nature* , *519* (7542), 171–180. https://doi.org/10.1038/nature14258

Liu, H., Lei, T. W., Zhao, J., Yuan, C. P., Fan, Y. T., & Qu, L. Q. (2011). Effects of rainfall intensity and antecedent soil water content on soil infiltrability under rainfall conditions using the run off-on-out method. *Journal of Hydrology* , *396* , 24–32. https://doi.org/10.1016/j.jhydrol.2010.10.028

Lobell, D. B., Thau, D., Seifert, C., Engle, E., & Little, B. (2015). Remote Sensing of Environment A scalable satellite-based crop yield mapper. *Remote Sensing of Environment* . https://doi.org/10.1016/j.rse.2015.04.021

Loureiro, S. M. C., & Gonzalez, F. J. M. (2008). The Importance of Quality, Satisfaction, Trust, and Image in Relation to Rural Tourist Loyalty. *Journal of Travel & Tourism Marketing* , *25* (2), 117–136. https://doi.org/10.1080/10548400802402321

Lu, D, & Weng, Q. (2007). A survey of image classification methods and techniques for improving classification performance. *International Journal of Remote Sensing* , *28* (5), 823–870. https://doi.org/10.1080/01431160600746456

Lu, Dengsheng, Tian, H., Zhou, G., & Ge, H. (2008). Remote Sensing of Environment Regional mapping of human settlements in southeastern China with multisensor remotely sensed data. *Remote Sensing of Environment* , *112* , 3668–3679. https://doi.org/10.1016/j.rse.2008.05.009

Mahlke, J. (1996). Characterization of Qklahoma Reservoir Wetlands For Preliminary Change Detection Mapping Using IRS- lB Satellite Imagery. *IEEE Transactions on Geoscience and Remote Sensing* , (405). https://doi.org/10.1109/IGARSS.1996.516795

Mayaux, P., Bartholome, E., Fritz, S., & Belward, A. (2004). A new land-cover map of Africa for the year 2000. *Journal of Biogeography* , *31* (6), 861–877. https://doi.org/10.1111/j.1365-2699.2004.01073.x

Metternicht, G. I., & Zinck, J. A. (2003). Remote sensing of soil salinity : potentials and constraints. *Remote Sensing of Environment* , *85* , 1–20. https://doi.org/10.1016/S0034-4257(02)00188-8

Miltner, A., Bombach, P., Schmidt-Brucken, B., & Kastner, M. (2012). SOM genesis: microbial biomass as a significant source.*Biogeochemistry* , *111* (1), 41–55. https://doi.org/10.1007/s10533-011-9658-z

Mougenot, B., Pouget, M., & Epema, G. F. (1993). Remote sensing of salt affected soils. *Remote Sensing Reviews* , *7* (3–4), 241–259. https://doi.org/10.1080/02757259309532180

Muir, J. F., Pretty, J., Robinson, S., Thomas, S. M., & Toulmin, C. (2010). Food Security : The Challenge of, *327* (February), 812–819. https://doi.org/10.1126/science.1185383

Pachepsky, Y. A., Guber, A. K., & Jacques, D. (2005). TEMPORAL PERSISTENCE IN VERTICAL DISTRIBUTIONS OF SOIL MOISTURE CONTENTS.*Soil Science Society of America Journal* , *69* , 347–352. https://doi.org/10.2136/sssaj2005.0347

Pampaloni, P., & Calvet, J. (2007). Operational readiness of microwave remote sensing of soil moisture for hydrologic applications.*Nordic Hydrology* , 1–20. https://doi.org/10.2166/nh.2007.029

Pope, P. T., & Webster, J. T. (1972). The Use of an F-Statistic in Stepwise Regression Procedures. *Technometrics* , *14* (2), 327–340. https://doi.org/10.1080/00401706.1972.10488919

Qadir, M., Ghafoor, A., & Murtaza, G. (2000). Amelioration strategies for saline soils: a review. *Land Degradation & Development* ,*11* (6), 501–521. https://doi.org/10.1002/1099-145X(200011/12)11:6<501::AID-LDR405>3.0.CO;2-S

Qadir, M., & Schubert, S. (2002). Degradation processes and nutrient constraints in sodic soils. *Land Degradation & Development* ,*13* (4), 275–294. https://doi.org/10.1002/ldr.504

Raina, R. S., Joseph, K. J., & Haribabu, E. (2010). and The Co-evolution of Exclusion in India Systems of Innovation for Inclusive Development : Lessons from Rural China and India. In *The 8th GLOBELICS International Conference* . Retrieved from https://s3.amazonaws.com/academia.edu.documents/42355672/Agricultural_Innovation_Systems_and_The_20160207-11053-kptho7.pdf?response-content-disposition=inline%3B filename%3DAgricultural_Innovation_Systems_and_the.pdf&X-Amz-Algorithm=AWS4-HMAC-SHA256&X-Amz-Credential=AKIAIWOWYYGZ2Y53UL3A%2F20200203%2Fus-east-1%2Fs3%2Faws4_request&X-Amz-Date=20200203T064008Z&X-Amz-Expires=3600&X-Amz-SignedHeaders=host&X-Amz-Signature=6ad828368138e146072471999dc1db67b9c7539ea13f8ea80873449397cf0d53

Rapp, A. (1986). Introduction to soil degradation processes in drylands.*Climatic Change* , *9* (1), 19–31. https://doi.org/10.1007/BF00140521

Rengasamy, P. (2010). Soil processes affecting crop production in salt-affected soils. *Functional Plant Biology* , *37* (7), 613–620. Retrieved from https://doi.org/10.1071/FP09249

Rengasamy, P., Chittleborough, D., & Helyar, K. (2003). Root-zone constraints and plant-based solutions for dryland salinity. *Plant and Soil* , *257* (2), 249–260. https://doi.org/10.1023/A:1027326424022

Reynolds, M., Kropff, M., Crossa, J., Koo, J., Kruseman, G., Milan, A. M., ... Vadez, V. (2018). Role of Modelling in International Crop Research : Overview and Some Case Studies. https://doi.org/10.3390/agronomy8120291

Rhoades, J. D. (1993). ELECTRICAL CONDUCTIVITY M ˜ THODS FOR M ˜ ASURING AND MAPPING SOIL SALINITY.*Advances in Agronomy* . https://doi.org/https://doi.org/10.1016/S0065-2113(08)60795-6

Rhoades, J. D., & Miyamoto, S. (1990, January 1). Testing Soils for Salinity and Sodicity. *Soil Testing and Plant Analysis* . https://doi.org/doi:10.2136/sssabookser3.3ed.c12

Rhoades, J. D., Shouse, P. J., Alves, W. J., Manteghi, N. A., & Lesch, S. M. (1990). Determining Soil Salinity from Soil Electrical Conductivity using Different Models and Estimates. *Soil Science Society of America Journal* , *54* (1), 46–54. https://doi.org/10.2136/sssaj1990.03615995005400010007x

Rhoades, J. D., & van Schilfgaarde, J. (1976). An Electrical Conductivity Probe for Determining Soil Salinity. *Soil Science Society of America Journal* , *40* (5), 647–651. https://doi.org/10.2136/sssaj1976.03615995004000050016x

Richardson, A. D., & Hollinger, D. Y. (2005). Statistical modeling of ecosystem respiration using eddy covariance data : Maximum likelihood parameter estimation , and Monte Carlo simulation of model and parameter uncertainty , applied to three simple models. *Agricultural and Forest Meteorology* , *131* , 191–208. https://doi.org/10.1016/j.agrformet.2005.05.008

Riffat, S. B., & Ma, X. (2003). Thermoelectrics : a review of present and potential applications. *Applied Thermal Engineering* ,*23* , 913–935. https://doi.org/10.1016/S1359-4311(03)00012-7

Ringler, C., Bhaduri, A., & Lawford, R. (2013). The nexus across water , energy , land and food (WELF): potential for improved resource use efficiency ? *Current Opinion in Environmental Sustainability* ,*5* (6), 617–624. https://doi.org/10.1016/j.cosust.2013.11.002

Saha, S. K. (2011). Microwave remote sensing in soil quality assessment.*International Archives of the Photogrammetry, Remote Sensing and Spatial Information Sciences, Volume XXXVIII-8/W20, 2011* ,*XXXVIII* (November). Retrieved from https://pdfs.semanticscholar.org/7f7a/0e28b81b726d1226f95c8664db3e00660829.pdf

SAHA, S. K., KUDRAT, M., & BHAN, S. K. (1990). Digital processing of Landsat TM data for wasteland mapping in parts of Aligarh District (Uttar Pradesh), India. *International Journal of Remote Sensing* ,*11* (3), 485–492. https://doi.org/10.1080/01431169008955034

Schmugge, T. J., Kustas, W. P., Ritchie, J. C., & Jackson, T. J. (2002). Remote sensing in hydrology. *Advances in Water Resources 25 (2002) 1367–1385* , *25* , 1367–1385. https://doi.org/10.1016/S0309-1708(02)00065-9

Shah, T., Molden, D., Sakthivadivel, R., & Seckler, D. (2001). Global Groundwater Situation: Opportunities and Challenges. *Economic and Political Weekly* , *36* (43), 4142–4150. Retrieved from http://www.jstor.org/stable/4411304

Sharma, R. C., Saxena, R. K., & Verma, K. S. (2000). Reconnaissance mapping and management of salt-affected soils using satellite images.*International Journal of Remote Sensing* , *21* (17), 3209–3218. https://doi.org/10.1080/014311600750019831

Shashi, T. A. and K. (2019). Effect of Phase Filtering on Interferometry based Displacement Analysis of Cultural Heritage Sites. In *2018 5th IEEE Uttar Pradesh Section International Conference on Electrical, Electronics and Computer Engineering (UPCON)* (pp. 1–5). IEEE. https://doi.org/10.1109/UPCON.2018.8597027

Shirvany, R. (2012). *Estimation of the Degree of Polarization in Polarimetric SAR Imagery: Principles & Applications* . University of Toulouse. Retrieved from http://ethesis.inp-toulouse.fr/archive/00002034/01/shirvany.pdf

Sowter, A., Bin, M., Amat, C., Cigna, F., Marsh, S., & Athab, A. (2016). Mexico City land subsidence in 2014 – 2015 with Sentinel-1 IW TOPS : Results using the Intermittent SBAS (ISBAS) technique.*International Journal of Applied Earth Observations and Geoinformation* , *52* , 230–242. https://doi.org/10.1016/j.jag.2016.06.015

Srivastava, H S, Patel, P., Sharma, Y., & Navalgund, R. R. (2009). Large-Area Soil Moisture Estimation Using Multi-Incidence-Angle RADARSAT-1 SAR Data. *IEEE Transactions on Geoscience and Remote Sensing* , *47* (8), 2528–2535. https://doi.org/10.1109/TGRS.2009.2018448

Srivastava, Hari Shanker, Patel, P., Prasad, S. N., Sharma, Y., Khan, B. A., & Praveen, B. (2008). Potential Applications of Multi-Parametric Synthetic Aperture Radar (Sar) Data in Wetland Inventory : A Case Study of Keoladeo National Park (A World Heritage and Ramsar Site), Bharatpur , India (Vol. 248001, pp. 1862–1879). Retrieved from https://s3.amazonaws.com/academia.edu.documents/35332826/Q-13.pdf?response-content-disposition=inline%3B filename%3DPotential_Applications_of_Multi-Para_met.pdf&X-Amz-Algorithm=AWS4-HMAC-SHA256&X-Amz-Credential=AKIAIWOWYYGZ2Y53UL3A%2F20200216%2Fus-east-1%2Fs3%2Faws4_request&X-Amz-Date=20200216T170722Z&X-Amz-Expires=3600&X-Amz-SignedHeaders=host&X-Amz-Signature=8108170de0e06844c4c21f81f28e66a9a165228c4edeedbe5dcfb0b837c7e7b8

Stenberg, B., Rossel, R. A. V., Mouazen, A. M., & Wetterlind, J. (2010). Visible and Near Infrared Spectroscopy in Soil Science. In*Advances in Agronomy* (1st ed., Vol. 107, pp. 163–215). Elsevier Inc. https://doi.org/10.1016/S0065-2113(10)07005-7

Streeter, J., & Wong, P. P. (1988). Inhibition of legume nodule formation and N2 fixation by nitrate. *Critical Reviews in Plant Sciences* , *7* (1), 1–23. https://doi.org/10.1080/07352688809382257

Susha Lekshmi, S., Singh, D., Tarantino, A., & Baghini, M. (2018). Evaluation of the Performance of TDR and Capacitance Techniques for Soil Moisture Measurement. *Geotechnical Testing Journal* , *41* (2), 292–306. https://doi.org/10.1520/GTJ20160240

Tapete, D., Cigna, F., & Donoghue, D. N. M. (2016). "Looting marks" in space-borne SAR imagery: Measuring rates of archaeological looting in Apamea (Syria) with TerraSAR-X Staring Spotlight. *Remote Sensing of Environment* , *178* , 42–58. https://doi.org/10.1016/j.rse.2016.02.055

Tiwari, A. T. and R. K. (2019). C-band SAR Interferometry based flood inundation mapping for Gorakhpur and adjoining areas. *IEEE XPLORE* .

Tripathi, A. and R. K. T. (2019). UTILIZATION OF SPACEBORNE C-BAND SAR DATA FOR ANALYSIS OF FLOOD UTILIZATION OF SPACEBORNE C-BAND SAR DATA FOR ANALYSIS OF FLOOD. In *ISPRS Archives* (pp. 2–6). https://doi.org/10.5194/isprs-archives-XLII-3-W6-521-2019

Tripathi, A., Kumar, S., & Maithani, S. (2018). Spaceborne bistatic polarimetrie SAR for scattering analysis and classification of man-made and natural features. In *2018 3rd International Conference on Microwave and Photonics, ICMAP 2018* (Vol. 2018-Janua). https://doi.org/10.1109/ICMAP.2018.8354494

Tripathi, Akshar. (2018). Effect of Phase Filtering on Interferometry based Displacement Analysis of Cultural Heritage Sites. *2018 5th IEEE Uttar Pradesh Section International Conference on Electrical, Electronics and Computer Engineering (UPCON)* , *1* , 1–5. https://doi.org/10.1109/UPCON.2018.8597027

Tripathi, Akshar, & Maithani, S. (2018). Spaceborne Bistatic Polarimetric SAR for Scattering Analysis and Classification of Man-made and Natural Features, (May), 10–12. https://doi.org/10.1109/ICMAP.2018.8354494

Tripathi, Akshar, & Tiwari, R. K. (2019a). Mapping of deflection caused due to hydrostatic pressure using Differential SAR Interferometry (DInSAR) on Bhakhra dam. *IEEE XPLORE* . https://doi.org/10.1109/UPCON47278.2019.8980117

Tripathi, Akshar, & Tiwari, R. K. (2019b). UTILIZATION OF SPACEBORNE C-BAND SAR DATA FOR ANALYSIS OF FLOOD. In *ISPRS Archives* (Vol. XLII, pp. 18–20).

Veci, L. (2016). SENTINEL-1 Toolbox SAR Basics Tutorial, (August).

Verhoest, N. E. C., Lievens, H., Wagner, W., Susan, M., Mattia, F., Sensing, R., ... Tejos, L. (2008). On the Soil Roughness Parameterization Problem in Soil Moisture Retrieval of Bare Surfaces from Synthetic Aperture Radar. *MDPI Sensors* , 4213–4248. https://doi.org/10.3390/s8074213

Viterbo, P., & Betts, A. K. (1999). Impact of the ECMWF reanalysis soil water on forecasts of the July 1993 Mississippi flood. *JOURNAL OF GEOPHYSICAL RESEARCH* , *104* (July 1993), 361–366. https://doi.org/https://doi.org/10.1029/1999JD900449

Vogt, J. V, Safriel, U., Von Maltitz, G., Sokona, Y., Zougmore, R., Bastin, G., & Hill, J. (2011). Monitoring and assessment of land degradation and desertification: Towards new conceptual and integrated approaches. *Land Degradation & Development* , *22* (2), 150–165. https://doi.org/10.1002/ldr.1075

Wagner, W., Lemoine, G., & Rott, H. (1996). A Method for Estimating Soil Moisture from ERS Scatterometer and Soil Data. *Remote Sensing of Environment* , *4257* (99). https://doi.org/https://doi.org/10.1016/S0034-4257(99)00036-X

Walker, J. P., Houser, P. R., & Willgoose, G. R. (2004). Active microwave remote sensing for soil moisture measurement : a fi eld evaluation using ERS-2. *Hydrological Processes* ,*1997* (February), 1975–1997. https://doi.org/10.1002/hyp.1343

Wymann von Dach S, Romeo R, Vita A, Wurzinger M, K. T. (eds). (n.d.).*Mountain Farming Is Family Farming* . https://doi.org/http://www.fao.org/docrep/019/i3480e/i3480e.pdf

Wymann von Dach S, Romeo R, Vita A, Wurzinger M, K. T. (eds). 2013. (2014). *Mountain Farming Is Family Farming Mountain Farming Is Family Farming A contribution from mountain areas to the International Year of Family Planning 2014* . Retrieved from https://boris.unibe.ch/46504/1/i3480e.pdf

Xie, J., Li, Y., Zhai, C., Li, C., & Lan, Z. (2009). CO2 absorption by alkaline soils and its implication to the global carbon cycle.*Environmental Geology* , *56* (5), 953–961. https://doi.org/10.1007/s00254-008-1197-0

Xie, Y., Sha, Z., & Yu, M. (2008). Remote sensing imagery in vegetation mapping: a review. *Journal of Plant Ecology* , *1* (1), 9–23. https://doi.org/10.1093/jpe/rtm005

Yang, H., Yang, X., Xu, X., Gao, Z., Li, C., Wang, J., & Zhao, C. (2011). Potential of Fully Polarimetric SAR Data for Crops Biophysical Parameters Retrieval.

Zhang, Y., Pulliainen, J., Koponen, S., & Hallikainen, M. (2002). Application of an empirical neural network to surface water quality estimation in the Gulf of Finland using combined optical data and microwave data. *Remote Sensing of Environment* , *81* , 327–336. https://doi.org/https://doi.org/10.1016/S0034-4257(02)00009-3

Zhou, T., Pan, J., Zhang, P., Wei, S., & Han, T. (2017). Mapping Winter Wheat with Multi-Temporal SAR and Optical Images in an Urban Agricultural Region, 1–16. https://doi.org/10.3390/s17061210